Available online at www.sciencedirect.com
SCIENCE DIRECT
Spectrochimica Acta Part A 64 (2006) 279–286
SPECTROCHIMICA ACTA PART A
www.elsevier.com/locate/saa

Infrared study of the acidic and basic forms of betaxolol

João Canotilho [b,*], R.A. Esteves de Castro [b], M. Helena [a], S.F. Teixeira [a], M. Luísa P. Leitão [a], J. Simões Redinha [a]

[a] *Chemistry Department, Rua Larga 3004-535, University of Coimbra, Portugal*
[b] *Faculty of Pharmacy, Rua do Norte 3000-295, University of Coimbra, Portugal*

Received 29 April 2005; received in revised form 28 June 2005; accepted 5 July 2005

Abstract

Betaxolol and its respective hydrochloride salt were studied in solution by computational calculations and infrared spectroscopy. The solution molecular conformations were taken to be the same as those exhibited by the compounds in the solid state given by X-ray diffraction and calculated after full geometry optimization by ab initio Hartree–Fock methods using the 6-31G(d) basis set. Infrared spectra of carbon tetrachloride solutions provide valuable information on the structure of the compounds in non-polar solvents at different concentrations.

Keywords: Ab initio calculations; IR spectroscopy; H-bonds; Betaxolol

1. Introduction

Many organic substances used as drugs contain molecular groups which are able to adopt acid–base behaviour according to the Brönsted concept. They can be administrated to the patients as free bases or as the more water soluble acid salts. Whatever the form in which the drug is ingested, a conjugate acid–base pair equilibrium is always established in the body. Thus, the study of the structure of the intervening compounds is of the utmost importance to the understanding of their biochemical behaviour.

The present work deals with betaxolol, (±)-1-{*p*-[2-(cyclopropylmethoxy) ethyl] phenoxy}-3-isopropylamino-2-propanol], and its hydrochloride salt (Fig. 1). It is a β-blocker agent used to treat arterial hypertension and intraocular hypertension [1].

A flexible backbone with a size similar to that of betaxolol and the presence of polar groups can give rise to diverse molecular conformations and to *intra-* and *inter*-molecular hydrogen bonds. The role played by the hydrogen bonding of a compound used for pharmaceutical applications is so important as to be the major structural feature that accounts for the biopharmaceutical classification of the drugs [2,3].

This research is based on the vibrational spectra calculated for the optimized molecular structure of the compounds under consideration and, in particular, on the infrared spectra determined in an inert solvent. The molecular conformation of both compounds was calculated by computational simulation from the data available from X-ray diffraction.

2. Materials and experimental procedures

Betaxolol (BT) was prepared by extraction from an alkaline solution of betaxolol hydrochloride (BTH) using methylene chloride as solvent. The organic phase was dried at 25 °C in a rotary vacuum evaporator. The original BTH was kindly supplied by Capsifar Ltd. and had a purity specification of 99.68 mol%. The harvested free base was analysed by HPLC, showing a 99.9 mol% purity.

Spectra of both BT and BTH dissolved in carbon tetrachloride were recorded in the 3800–2200 cm^{-1} region. Carbon tetrachloride for infrared spectrometry, purchased from Fluka, was used for the preparation of the solutions. Solutions of different concentrations were prepared and the spectra traced with a Thermo Nicolet IR 300 spectrometer. A

* Corresponding author. Tel.: +351 239859950; fax: +351 239827126.
E-mail address: jcano@ci.uc.pt (J. Canotilho).

1386-1425/$ – see front matter © 2005 Elsevier B.V. All rights reserved.
doi:10.1016/j.saa.2005.07.021

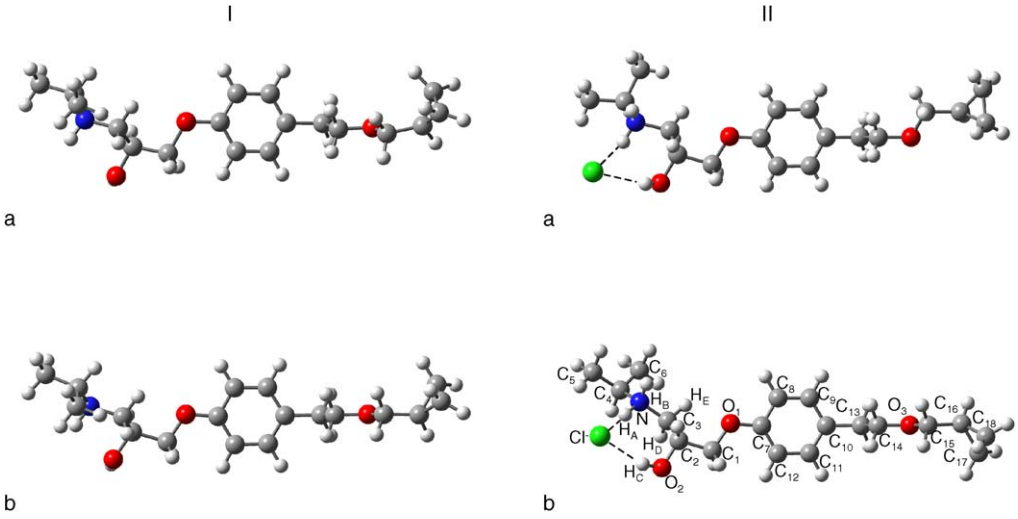

Fig. 1. Molecular conformations: I, isolated molecule (a) and relaxed isolated molecule (b) for BT; II, isolated molecule (a) and relaxed molecule (b) for BTH.

3.48 mm pathlength cell with sodium chloride windows was used. The spectra are shown in Fig. 4.

3. Discussion

X-ray diffraction data are the only information on the structure of BT and BTH available for these compounds. As it is not easy to map the lower energy conformers present in solution for flexible molecules with size like those of betaxolol, the molecular conformation in the solid state is used as the starting-point to determine its conformation in solution. Indeed, allowing for molecular packing restraints, the interaction between the polar groups and the solvent gives rise to a conformation identical to that obtained from intermolecular interactions in the solid state. The packing effect is corrected, at least in part, by the relaxation of the molecular structure in the solid state.

From the X-ray fractional coordinates given for BT [4] and BTH [5], the isolated molecule retaining the solid state conformation was built for each compound. As X-ray does not give the hydrogen position, these atoms were added automatically. The program used was Cerius^2 Version 3.5 supplied by Molecular Simulation Inc. running in a Silicon Graphics O^2/RS 5000 workstation. The molecule isolated from the crystal structure but retaining its original conformation was fully optimized at the HF/6-31G* level of theory. The isolated molecule, before and after optimization, is differentiated hereafter by calling the former *isolated molecule* and the latter *relaxed isolated molecule*. In Fig. 1, the structures of conformations for BT and BTH are represented and Table 1 gives the values corresponding to the structural parameters.

As one can see from the parameters given in Table 1, the BT and BTH molecules both have a fully distended backbone. Very little deviation from this conformation is observed when the isolated molecule is free to relax. The major deviation is observed for the $C_{13}C_{14}O_3C_{15}$ dihedral angle in BTH. In the relaxed isolated molecule, the value found for this angle is 50° towards the gauche side relative to the conformation of the isolated molecule. This molecular moiety has no polar groups and therefore cannot participate in interactions other than those due to van der Waals intermolecular forces. A certain mobility of this side chain by rotation around the (C_{15}–C_{16}) bond was in fact shown by X-ray diffraction [5].

The isopropilamino-2-propanol moiety may play a major role in the structure of the β-blockers under study because it contains polar groups capable of specific interactions. From the values tabled for the structural factors of the relaxed isolated molecule of BT, the only possible intramolecular interaction is that between the amine and hydroxyl groups. Although the value of $d(H_A\cdots O_2)$ is shorter than the sum of the van der Waals radii of the two atoms and within the interval accepted for a hydrogen bond [6,7], the (N^+–H_A) direction is not favourable to the formation of this bond. Thus, no significant internal interaction can be assigned in the relaxed isolated molecule.

The molecular conformation in BTH is strongly dominated by the interactions of the (O_3–H_C) group with Cl^- and of (N^+–H_A) with the same anion. Chloride ion is in fact considered a hydrogen bond acceptor from a number of molecular groups, in particular from OH and NH [8–10]. The values found for $d(H_C\cdots Cl^-)$ and for $<(O_3H_2Cl^-)$ indicate the existence of a favourable hydrogen bond direction compared with the value given in the surveys delivered by some authors [11,12]. The electrostatic interaction between the two ions takes place through the H_A atom. Indeed, the attraction of the H_A atom by the Cl^- shortens the ($H_A\cdots Cl^-$) distance and distends the (N^+–H_A) bond. That is, the interaction with the ammonium ion can be described as a hydrogen bond strengthened by the ion-pair interaction.

The seven membered ring formed by the two hydrogen bonds involving Cl^- is an important feature of the structure of the BTH molecule. To reach a favourable conformation for the simultaneous interaction of (O_3–H_C) and (N^+–H_A) with

Table 1
Values of the angles and distances for the molecular conformation of the isolated molecule and of the relaxed molecule of BT and BTH

	BT		BTH	
	Isolated molecule	Relaxed molecule	Isolated molecule	Relaxed molecule
Dihedral angles (°)				
$C_2C_1O_1C_7$	−160.7	−179.8	−177.1	178.0
$O_2C_2C_1O_1$	176.4	175.4	−177.6	−178.2
$C_1C_2C_3N$	176.3	176.5	179.6	−160.2
$C_2C_3NC_4$	−161.2	−173.0	−172.9	−160.7
$C_{13}C_{14}O_3C_{15}$	−178.8	−179.8	124.5	−179.9
$C_{14}O_3C_{15}C_{16}$	−169.6	178.0	−177.5	−178.0
$C_1C_2O_2H_C$	−98.1	−83.1	134.5	158.2
$C_1C_2C_3H_D$	−63.7	−58.9	59.9	81.3
$C_2C_3NH_A$	73.9	61.0		
$C_2C_3N^+H_A$			−53.1	−37.7
$C_2C_3N^+H_B$			67.3	75.2
Distances (Å)				
$d(H_A\cdots Cl^-)$			2.44	1.99
$d(H_C\cdots Cl^-)$			2.33	2.29
$d(O_2–H_C)$	0.96	0.95	0.85	0.96
$d(O_2\cdots N)$	2.91	2.82		
$d(O_2\cdots N^+)$			2.92	3.14
$d(O_2\cdots H_A)$	2.71	2.48	2.50	2.80
$d(N–H_A)$	1.00	1.00		
$d(N^+–H_A)$			1.00	1.04
$d(N^+–H_B)$			–	–
$d(O_1\cdots H_E)$	2.55	2.61	2.53	2.43
$d(O_1\cdots C_3)$	2.96	2.95	2.86	2.86
Angles (°)				
$<(Cl^-H_AN^+)$			160.5	173.2
$<(Cl^-H_CO_2)$			166.0	155.5
$<(NH_AO_2)$	91.4	99.6		
$<(N^+H_AO_2)$			104.3	99.2
$<(C_3H_EO_1)$	102.3	95.6	100.1	102.2

Cl^-, the isopropilamine-2-propanol moiety in BTH results from that of BT by a rotation around the (C_3–C_2) bond.

The type of structure just described for the relaxed isolated molecule was also found in crystalline BTH [5] and was put forward to interpret the results obtained by ^{1}H NMR and IR spectroscopy for hydrohalide salts of β-blockers dissolved in aprotic non-polar solvents [12].

The ion-pair structure of the relaxed isolated molecule described above raises the question of whether it corresponds to the structure of BTH in gas state or is simply the structure of the isolated molecule existing in liquid media. Extensive work has been done on the nature of the products formed from the reaction of ammonia and some alkyl-derivatives with hydrogen chloride in gas phase. Ab initio computational methods applied to the study of the reaction between ammonia and hydrogen chloride indicate that, for greater distances, the mutual polarization of both molecules with hydrogen bonding formation occurs. However, as HCl gets closer to NH_3, a hydrogen transfer with ($NH_4^+Cl^-$) ion-pair formation takes place [13,14]. Using data obtained by rotational spectroscopy, Legon [15] proved that the proton transfer from the hydrogen chloride molecule to the nitrogen atom increases progressively with methylation of the ammonia. In the gaseous system formed by trimethylammine and hydrogen chloride, the ionic character of the reaction product is about 67%.

In the case of BTH, the hydrogen bond between (O_3–H_C) and Cl^- reinforces the ion-pair interaction between the chloride and the ammonium ions. Hence, the ion-pair is really a significant structure of BTH in gas phase.

Valuable information on the structure, particularly on hydrogen bonding, can be gathered from vibrational spectra. Accordingly, let us now consider the spectra calculated for the relaxed isolated molecule. Vibrational modes were calculated in the 3800–2300 cm^{-1} interval for BT with the level of theory used in the structure optimization. The wavenumbers scaled by the conventional factor of 0.8929 [16] are given in Table 2 and the spectra are given in Fig. 2. Gauss View animation was used to assign the bands.

In the 3700–3038 cm^{-1} region, BT exhibits an intense band at 3678 cm^{-1}, which is due to the free OH group. This value is a little above the wavenumber interval 3650–3600 cm^{-1} tabled for this group. This fairly common discrepancy is attributed to the overestimated molecular polarity in the HF method, resulting from neglecting electron correlation [17]. The vanishing weak band at 3359.9 cm^{-1} corresponds to the free NH group. No evidence is found for the presence of an ($N–H\cdots O_2$) hydrogen bond, which agrees

Table 2
Wavenumbers, intensities and approximate description of calculated absorption bands for BT and BTH

BT			BTH		
ν (cm^{-1})	I (km mol^{-1})	Description	ν (cm^{-1})	I (km mol^{-1})	Description
3678.4	60.1	$\nu(O_2H)$	3481.1	633.4	$\nu(O_2H)$
3359.9	2.9	ν(NH)			
			3313.9	32.7	$\nu(NH_B)$
			3039.6	12.1	$\nu(C_{12}H)$
3038.2	15.0	$\nu(C_{12}H)$	3031.6	39.7	$\nu_a(C_{17}H_2)$, $\nu_a(C_{18}H_2)$ i.p.
3031.2	40.1	$\nu_a(C_{17}H_2)$, $\nu_a(C_{18}H_2)$ i.p.			
3027.4	10.6	$\nu(C_8H)$, $\nu(C_9H)$ i.p.	3024.3	13.8	$\nu(C_8H)$, $\nu(C_9H)$ i.p.
3016.6	1.6	$\nu_a(C_{17}H_2)$, $\nu_a(C_{18}H_2)$ o.p.	3017.1	1.4	$\nu_a(C_{17}H_2)$, $\nu_a(C_{18}H_2)$ o.p.
			2997.3	21.4	$\nu(C_{11}H)$
			2995.4	17.1	$\nu(C_9H)$
			2994.6	8.4	$\nu_a(C_3H_2)$
2994.4	23.1	$\nu(C_9H)$, $\nu(C_{11}H)$ i.p.			
2993.8	19.9	$\nu(C_9H)$, $\nu(C_{11}H)$ o.p.			
2975.7	12.4	$\nu(C_{16}H)$	2975.7	12.5	$\nu(C_{16}H)$
			2964.3	2.3	$\nu_a(C_5H_3)$
2958.2	19.7	$\nu_s(C_{17}H_2)$, $\nu_s(C_{18}H_2)$ i.p.	2958.4	19.5	$\nu_s(C_{17}H_2)$, $\nu_s(C_{18}H_2)$ i.p.
			2950.3	31.1	$\nu_s(C_{17}H_2)$, $\nu_s(C_{18}H_2)$ o.p.
2949.9	31.5	$\nu_s(C_{17}H_2)$, $\nu_s(C_{18}H_2)$ o.p.			
			2947.7	27.6	$\nu_a(C_6H_3)$
			2941.6	50.4	$\nu_a(C_5H_3)$, $\nu_a(C_6H_3)$ i.p., $\nu(C_4H)$
			2936.2	32.9	$\nu_a(C_1H_2)$
2933.9	42.8	$\nu_a(C_6H_3)$	2930.6	1.3	$\nu_s(C_3H_2)$
			2925.7	3.1	$\nu_a(C_5H_3)$, $\nu_a(C_6H_3)$ o.p.
2921.6	44.9	$\nu_a(C_5H_3)$, $\nu_a(C_3H_2)$ o.p.			
2919.7	63.3	$\nu_a(C_5H_3)$, $\nu_a(C_3H_2)$ i.p.	2917.9	8.2	$\nu_a(C_5H_3)$, $\nu_a(C_6H_3)$ i.p., $\nu(C_4H)$
			2917.4	31.5	$\nu_a(C_{13}H_2)$
2916.1	32.6	$\nu_a(C_{13}H_2)$			
2911.3	102.6	$\nu_a(C_5H_3)$, $\nu_a(C_6H_3)$ i.p., $\nu(C_4H)$			
2905.8	69.5	$\nu_a(C_1H_2)$, $\nu(C_2H)$			
2900.2	1.8	$\nu_a(C_5H_3)$, $\nu_a(C_6H_3)$ o.p.			
2887.5	8.0	$\nu_a(C_1H_2)$, $\nu(C_2H)$	2879.7	37.5	$\nu_s(C_{13}H_2)$
2878.6	38.3	$\nu_s(C_{13}H_2)$	2877.8	41.2	$\nu_s(C_1H_2)$, $\nu(C_2H)$
			2869.5	19.4	$\nu_s(C_6H_3)$, $\nu_s(C_5H_3)$ i.p.
			2868.7	6.1	$\nu_s(C_1H_2)$, $\nu(C_2H)$
			2863.6	11.5	$\nu_s(C_6H_3)$, $\nu_s(C_5H_3)$ o.p.
2857.9	55.2	$\nu_s(C_6H_3)$, $\nu_s(C_5H_3)$ i.p., $\nu(C_4H)$			
2857.4	32.0	$\nu_s(C_1H_2)$			
2855.5	12.2	$\nu_s(C_6H_3)$, $\nu_s(C_5H_3)$ i.p., $\nu(C_4H)$			
2852.3	84.2	$\nu_a(C_{14}H_2)$, $\nu_a(C_{15}H_2)$ i.p.	2852.5	92.1	$\nu_a(C_{14}H_2)$, $\nu_a(C_{15}H_2)$ i.p.
2850.1	24.4	$\nu_s(C_6H_3)$, $\nu_s(C_5H_3)$ o.p.	2847.0	19.1	$\nu_a(C_{14}H_2)$, $\nu_a(C_{15}H_2)$ o.p.
2845.8	26.6	$\nu_a(C_{14}H_2)$, $\nu_a(C_{15}H_2)$ o.p.			
2830.9	83.3	$\nu_s(C_{14}H_2)$, $\nu_s(C_{15}H_2)$ i.p.	2831.3	84.1	$\nu_s(C_{14}H_2)$, $\nu_s(C_{15}H_2)$ i.p.
2816.9	10.2	$\nu_s(C_{14}H_2)$, $\nu_s(C_{15}H_2)$ o.p.	2817.7	9.3	$\nu_s(C_{14}H_2)$, $\nu_s(C_{15}H_2)$ o.p.
2810.9	43.3	$\nu_s(C_3H_2)$	2703.4	1534.3	$\nu(NH_A)$

with the conclusion drawn from the geometric parameters calculated for the relaxed isolated molecule.

A feature to be noted in the calculated spectra is the difference between the values found for the *anti-* and *symmetric* (C–H) stretch of (C_3H_2). The difference between the two vibration modes is markedly higher than those observed for the other groups. The explanation lies in the influence of the non-bonding electron pair of the nitrogen atom. The decrease of the electronic charge on H_D atom under the influence of the electron pair leads to a rather low value of $\nu_s(C_3H_2)$. The non-bonding electron pair turns the hydrogens of (C_3H_2) into non-equivalent atoms. Thus, the main contribution to the *anti–symmetric* stretching intensity comes from (C_3–H_E), whilst for the symmetric mode, (C_3–H_D) is the main

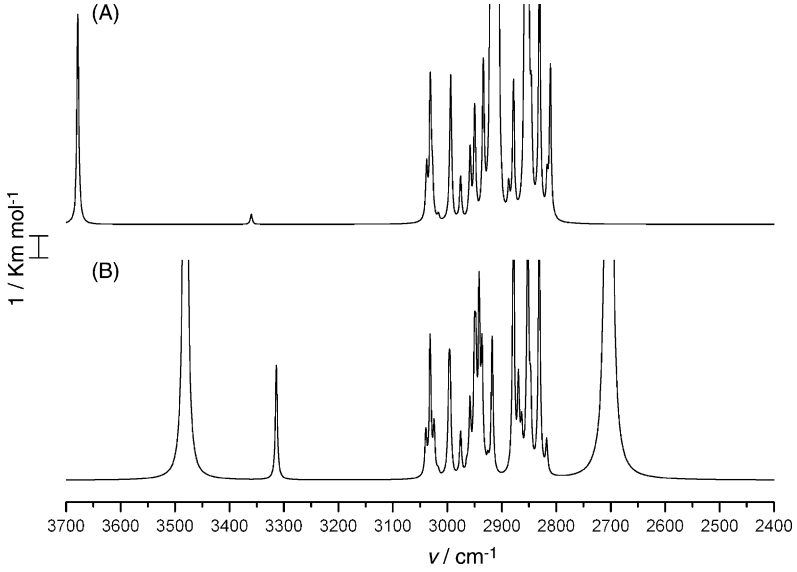

Fig. 2. Vibrational spectra calculated for the relaxed isolated molecule for: (A) BT and (B) BTH.

contributor. Such an effect does not occur in BTH as the nitrogen is now under the ammonium ion structure.

The spectrum pattern of BTH corresponding to the (C–H) stretching vibration is identical to that given for BT. However, differences between the spectra of both, at either higher or lower wavenumbers, should be pointed out. On the higher wavenumber side, a band ascribed to (O_2–H) at 3481.1 cm^{-1} and another corresponding to (N–H_B) at 3313.9 cm^{-1} are observed. The red shift of 197 cm^{-1} for the (O–H) stretch vibration mode indicates the participation of the group in hydrogen bonding with the chloride ion. On the lower wavenumber side, the striking difference between the spectra of the acid and base forms is observed in the 2817.7–2703.4 cm^{-1} interval. In this region, no absorption is registered for BT whilst a strong band is observed in the BTH spectrum at 2703.4 cm^{-1}. This band corresponds to the (N–H_A) group acting as hydrogen donor to chloride ion.

The spectra of the compounds dissolved in a non-polar solvent provide data in support of conclusions drawn from computational calculations and to obtain complementary information on the molecular structure under investigation. Fig. 3 gives the spectra of BT and BTH in different concentrations of carbon tetrachloride solutions.

In very dilute solutions, the BT spectra show a band at $\nu_{max} = 3625\ cm^{-1}$ which corresponds to the stretching of the free OH group and a set of several overlapped bands at

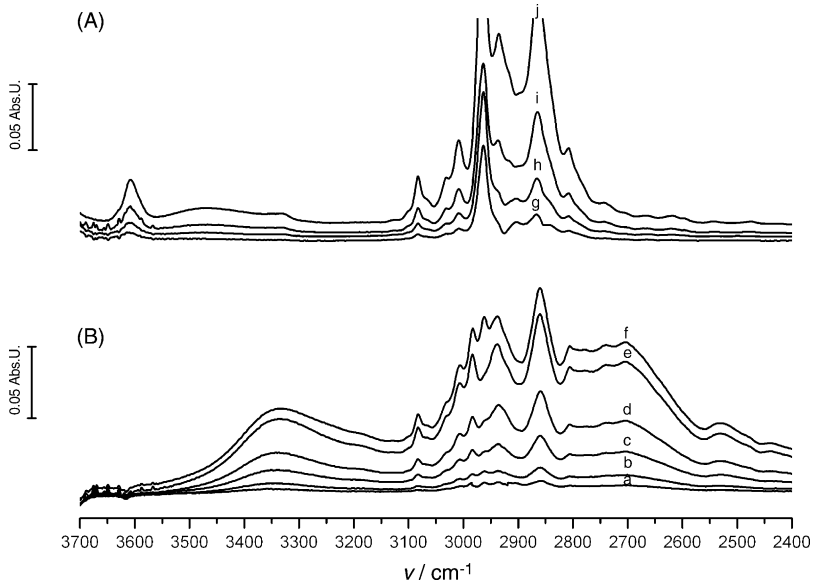

Fig. 3. IR spectra of BT (A) and BTH (B) in CCl_4 solution at different concentration ranges: (a) 0.04 mM; (b) 0.12 mM; (c) 0.24 mM; (d) 0.38 mM; (e) 0.83 mM; (f) 1.06 mM; (g) 0.25 mM; (h) 0.50 mM; (i) 1.03 mM; (j) 1.99 mM.

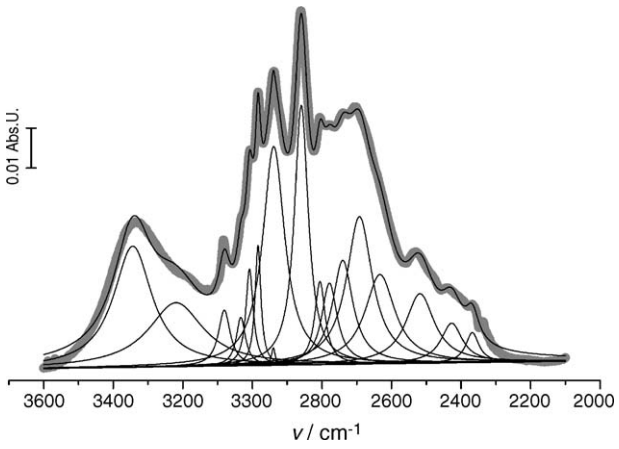

Fig. 4. Curve-fitting of spectra of BTH 0.83 mM in CCl_4 solution.

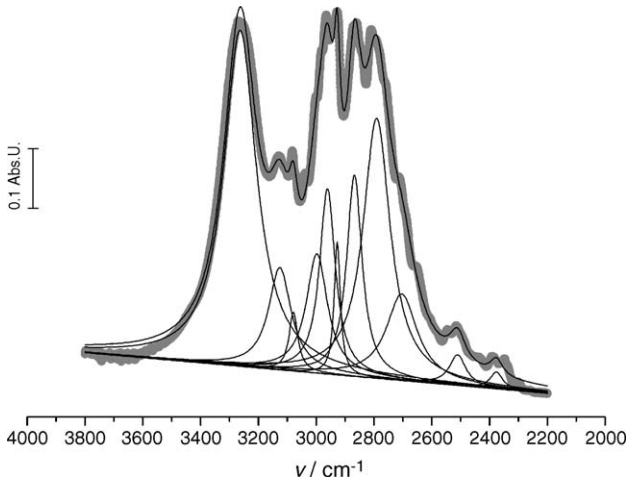

Fig. 5. Curve-fitting of spectrum recorded for the solid BTH.

3100–2800 cm^{-1}, due to the stretching vibration of (C–H) groups. This spectrum pattern was expected, on the basis of that calculated for the relaxed isolated molecule. Thus, in very dilute solutions, free BT molecules are the solute units present in solution. As the concentration increases, a broad absorption band is observed at 3550–3300 cm^{-1}, due to intermolecular hydrogen bonds. This means that self-association of BT molecules in non-polar media takes place at concentrations higher than 0.5 mM and concomitantly with monomer there are multimers resulting from self-association in solution.

The spectra of BTH in carbon tetrachloride presented in Fig. 3B indicate that the hydroxyl group is not free at concentrations as low as 0.04 mM. We did not expect this behaviour unless the interaction between (O_5H_C) and Cl^- present in the isolated molecule was no longer present in solution. However, the broad band observed in the spectra cannot be interpreted simply as due to that interaction; it is, rather, the manifestation of a more complex intermolecular hydrogen bonding. That is, in the range of concentrations studied, BTH molecules are associated however low the concentration, giving rise to molecular aggregates.

Attempting to go further into the structure of these aggregates, the overlapped absorption bands between 3600 and 2100 cm^{-1} were decomposed into component bands by peak-fitting analysis. The Origin® Version 7 program was used to fit the spectra to Lorentzian functions. A typical curve fit analysis is shown in Fig. 4.

Two regions have particular interest for structural aspects. The first is that between 3600 and 3100 cm^{-1} where intermolecular hydrogen bonds involving the polar groups occur. The second, between 2800 and 2300 cm^{-1} where, according to the calculated spectrum, the (N^+–H_A···Cl^-) will be localized.

The comparison of the spectra of the molecular aggregates in solution with that of the solid state favours their interpretation, the more so because the solid structure is known. The stretching vibration spectrum recorded for solid BTH using the KBr technique is presented in Fig. 5.

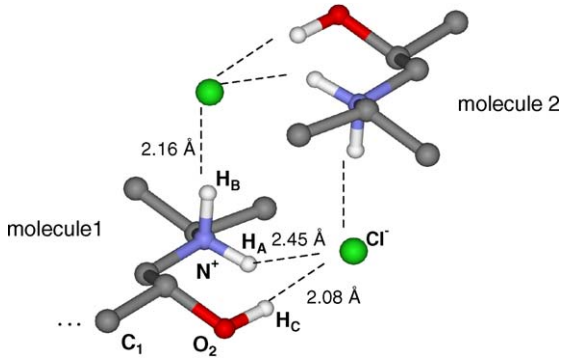

Fig. 6. Detail of the hydrogen bond network of betaxolol hydrochloride in the solid state. The diagram contains only the molecular groups involved in *intra*- and *inter*-molecular bonds.

Fitting analysis allows assignment of bands at 3263.2 and 3125.7 cm^{-1} in the first region and four bands in second. The main absorption band in the latter region is at $\nu_{max} = 2790.6\ cm^{-1}$. The comparison between the spectra of the solid and those of the aggregates proves that they have a similar structure. As the multimers grow and we are getting close to the crystalline state, a shift of bands from the first region towards lower wavenumbers and from the second towards larger wavenumbers is observed.

Based on the data supplied by X-ray diffraction [5], a diagram of the hydrogen bonding system existing in BTH is shown in Fig. 6 and the characteristic parameters of these bands are given in Table 3. Besides the bonds

Table 3
Metrics related to *intra*- and *inter*-molecular H-bonds in crystalline BTH

Hydrogen bond D–H···A	H···A distance (Å)	DHA angle (°)
N^+–$H_A(1)$···$Cl^-(1)$	2.45	160.5
N^+–$H_B(1)$···$Cl^-(2)$	2.16	177.2
O_2–$H_C(1)$···$Cl^-(1)$	2.08	166.0

considered in Fig. 6, some authors mention a short distance between (N^+–H_A) group and the O_2 of a neighbour molecule (molecule 3). However, the geometric parameters are not favourable to a hydrogen bond of significant strength.

The main interactions in which a molecule in the BTH crystal is involved are: two hydrogen bonds between the (N^+–H_A) and the (O_2–H_C) groups with a chloride ion, a third hydrogen bond between this chloride ion and (N^+–H_B) of another molecule (molecule 2) and a fourth hydrogen bond equivalent to the last one between (N^+–H_B) and the chloride ion of the molecule 2. Three distinct bands in the BTH spectrum as well as in those of the molecular aggregates are expected.

The comparison of the values given for the structural parameters of the relaxed isolated molecule and for the crystal helps the assignment of the bands to the molecular groups. Going from the molecular optimized structure to the crystal, the (N^+–H_A···Cl^-) distance increases significantly whilst that for (O_2H_C···Cl^-) decreases. The ($N^+H_ACl^-$) and ($O_2H_CCl^-$) angles both became less favourable to the formation of hydrogen bonds. In the molecular optimized structure, the interatomic distances and the angles related to H-bonding indicate that (N^+H_A···Cl^-) is stronger than the (O_2H_C···Cl^-) bond; in the crystal, an opposite situation is observed. On the other hand, the intermolecular (N^+–$H_B(1)$···$Cl^-(2)$) bond is, of all hydrogen bonds in the crystalline BTH structure, the one with the shorter donor–acceptor distance and a more favourable direction. The absorption at $\nu_{max} = 2790.7\,cm^{-1}$ should therefore correspond to this bond. The two others have the following assignments: $3126\,cm^{-1}$ to (O_2–H_C···Cl^-) and $3263\,cm^{-1}$ to (N^+–H_A···Cl^-). The three hydrogen bonds assigned to the BTH crystal also constitute the frame of the intermolecular interactions in the aggregates formed in non-polar solvents.

It is worth comparing the intensities of the bands ascribed to the OH and NH groups with those corresponding to (C–H) groups, in the transition from the molecular aggregates in solution to the crystalline solid. The intensity of the bands for the polar groups increase relative to those of the non-polar ones, giving rise to different spectra profiles. The cooperative effect very likely reinforces the intermolecular hydrogen bonds.

The study has so far looked at the structure of the compounds under consideration in the gas state and in non-polar solvents. It is also important to have information on the structure of these compounds in polar solvents. General structural features in these solvents can be predicted from the properties displayed in the other media. As the distended backbones attained by the BT and BTH molecules in non-polar media are favourable to interactions between the polar groups and the polar solvent molecules, it is very likely that no significant change will take place on changing from non-polar to polar solvents.

The most important change in the structure will take place in BTH when we move from non-polar to polar solvents. The increase of the dielectric constant stabilises the isolated charges and dipoles. Moreover, the interaction between the polar groups of the solute – in particular the ammonium ion and chloride ion – renders self-association more difficult. For this reason, BTH in polar solvents is dissociated into hydrogen BT ion and chloride ion as free ions. In fact, the value obtained for the acid–base equilibrium constant in aqueous solutions in the presence of Cl^-, considered as good hydrogen bond acceptor, is the same as that obtained in the presence of NO_3^- or ClO_4^- [18], which do not have this ability.

4. Conclusions

The molecular conformations of betaxolol and betaxolol hydrochloride in dilute solutions were obtained by computational simulation from the data available for the crystalline structure. This made it possible to take advantage of the computational calculation, and in conjunction with experimental methods, allowed a deep insight into condensed matter states.

From the vibrational frequencies calculated for the optimized molecular structure and for the compounds dissolved in carbon tetrachloride, the role played by hydrogen bonding in the structure of the acidic and basic form of betaxolol was revealed.

The information given by infrared spectroscopy together with the characterization provided valuable data on betaxolol, both from the structural viewpoint and with respect to its pharmaceutical and clinical use.

References

[1] G. Caron, P. Gaillard, P.A. Carrupt, B. Testa, Helv. Chim. Acta 80 (1997) 449.
[2] G.L. Amidon, H. Lennernäs, V.P. Shah, J.R. Crison, Pharm. Res. 12 (1995) 413.
[3] H.V. Waterbeemed, Eur. J. Pharm. Sci. 7 (1998) 1.
[4] Work carried out in this Research Center to be published elsewhere.
[5] P.G. Mairesse, J.C. Boivin, D.J. Thomas, Acta Cryst. C40 (1984) 1432.
[6] G.R. Desiraju, T. Steiner, The Weak Hydrogen Bond in Structural Chemistry and Biology, Oxford University Press, Inc., New York, 1999 (Chapter 1).
[7] T. Steiner, Chem. Commun. 8 (1997) 727.
[8] G.R. Desiraju, T. Steiner, The Weak Hydrogen Bond in Structural Chemistry and Biology, Oxford University Press Inc., New York, 1999 (Chapter 3).
[9] L. Brammer, E.A. Burton, P. Sherwood, Cryst. Growth Des. 1 (2001) 727.
[10] T. Steiner, Acta Cryst. B54 (1998) 456.
[11] M.J. Mascal, J. Chem. Soc. Perkin Trans. 2 (1997) 1999.
[12] J. Zaagsma, J. Med. Chem. 22 (1979) 441.
[13] E. Clementi, J. Chem. Phys. 46 (1967) 3851.
[14] G. Corongin, D. Estrin, G. Murgia, L. Paglieri, L. Pisani, G.S. Valli, J.D. Watts, E. Clementi, Int. J. Quantum Chem. 59 (1996) 119.
[15] A.C. Legon, Chem. Soc. Rev. 3 (1993) 153.
[16] M.J. Frisch, G.W. Trucks, H.B. Schlegel, G.E. Scuseria, M.A. Robb, J.R. Cheeseman, V.G. Zakrzewski, J.A. Montgomery Jr., R.E. Stratmann, J.C. Burant, S. Dapprich, J.M. Millam, A.D. Daniels, K.N. Daniels, K.N. Kudin, M.C. Strain, O. Farkas, J. Tomasi, V. Barone,

M. Cossi, R. Cammi, B. Mennucci, C. Pomelli, C. Adamo, S. Clifford, J. Ochterski, G.A. Petersson, P.Y. Ayala, Q. Cui, K. Morokuma, D.K. Malick, A.D. Rabuck, K. Raghavachari, J.B. Foresman, J. Cioslowski, J.V. Ortiz, B.B. Stefanov, G. Liu, A. Liashenko, P. Piskorz, I. Komaromi, R. Gomperts, R.L. Martin, D.J. Fox, T. Keith, M.A. Al-Laham, C.Y. Peng, A. Nanayakkara, C. Gonzalez, M. Challacombe, P.M.W. Gill, B. Johnson, W. Chen, M.W. Wong, J.L. Andres, C. Gonzalez, M. Head-Gordon, E.S. Replogle, J.A. Pople, GAUSSIAN 98, Revision A.9, Gaussian, Inc., Pittsburgh, PA, 1998.

[17] Y.A. Abramov, A. Volkov, G. Wu, P. Coppens, J. Phys. Chem. B 104 (2000) 2183.

[18] Data obtained by the authors to be published elsewhere.